A Reliable Technique for Power Generation Enhancement in Unsymmetrical PV Arrays during Partial Shading

Belqasem Aljafari
Department of Electrical Engineering
Najran University
Najran 11001, Saudi Arabia
bhaljafari@nu.edu.sa

Sudhakar Babu Thanikanti
Department of EEE
CBIT
Hyderabad 500075, India
sudhakarbabu66@gmail.com

Karthik Balasubhramanian
DeGroote School of Business
McMaster University
Ontario, Canada
balask8@mcmaster.ca

***Abstract*—Solar Photovoltaic (PV) arrays consist of modules that are connected to generate the power required by the loads. The arrays are expected to generate the maximum power based on the irradiance at the site but, in the field, this condition gets affected by the frequently occurring partial shading. The effect of partial shading is so large that it can reduce the power output of the arrays to zero and creates complications such as hotspots in modules, power losses, and distorted power curves. To overcome these complications, this paper proposed a reliable technique that uses a switching matrix circuit to effectively distribute the current in the array under partial shading. The proposed switching matrix determines the optimal electrical connection of the modules based on the minimum row current difference approach which is calculated using the particle swarm optimization algorithm to enhance the power output of the PV array during partial shading. The system has been tested for a 7x4 unsymmetrical array that uses 56 switches to reduce the losses in the array and enhance the power during partial shading. The investigation is conducted in MATLAB simulation and the proposed system is compared with conventional, hybrid, and existing static reconfiguration techniques under partial shading. The analysis conducted shows that the proposed system has 53.95%, 46.2%, 45.9%, 26.3%, and 20.94% of average power improvement than the SP, TCT, SP-TCT, SDS, and FER respectively.**

Keywords—photovoltaic, switching matrix, genetic algorithm, partial shading, power losses

I. INTRODUCTION

Partial shading occurs frequently in the operating site of the solar PV arrays that cannot be avoided in any way [1]. In the case of roof-top systems and large power plants, shadows of nearby buildings and trees, bird droppings, dust, clouds, snow, and self-shading are the major causes of partial shading among the modules as shown in Fig.1 [2]. Partial shading in the PV system leads to different irradiances in the modules and thus to unequal operating conditions, which result in power losses in the system and hotspots [3]. In practice, bypass diodes are installed anti-parallel with the modules to bypass the higher current through the shaded modules and hence, prevent the PV modules from hotspots and losses in the system [4]. But this solution creates additional complication by deteriorating the characteristics curves of the PV arrays with larger maximum power points (MPPs) [5]. Hence, with the distorted curves, the conventional maximum power point trackers (MPPT) get converged to the first peak as the maximum power even if the actual maximum power lies at the other peaks of the curve [6, 7]. However, to deal with this fault tracking issue, the researcher proposed various advanced MPPT algorithms in the wide range of literature that uses optimization algorithms such as swarm intelligence [8], and nature-inspired [9] techniques to locate the position of the actual peak with maximum power value. But, the practical implementation of these techniques still has various demerits such as expensive and complexities due to the microcontroller requirement and related algorithms.

In recent years, array reconfiguration is playing a vital role in partial shading mitigation due to merits such as higher reliability, inexpensive, and reduced complexities [10]. The reconfiguration is classified into two categories i.e., static and dynamic whose implementation differs from each other but the concept remains the same. In static approach, the modules of the array are repositioned to different locations than the actual position based on shade dispersion algorithms. Some examples of static techniques include SDS [11], FER [12], henon map [13], ancient Chinese magic square [14], SDP [15], SD-PAR [16], Triple X sudoku [17], ER [18], hyper sudoku [19], ZSSR [20], two-Step module placement [21], modified Sudoku [22], and electrical reconfiguration [23].

Fig. 1. Potential causes of partial shading in PV arrays [Source: Google]

These techniques are one-time fixed arrangements of the modules and do not require any additional components such as switches and sensors for operation and power enhancement. But the major limitation lies in the proper shade dispersion, lower power enhancement, and unreliable operation during all shading situations. Hence, to solve this limitation, the dynamic reconfiguration approach came into existence that utilizes the switches, sensors, and some algorithms like fuzzy logic [24], dragonfly [25], Pareto optimization [26], and modified harris hawk's optimizer [27] algorithms for proper shade dispersion and power enhancement in the arrays during partial shading. But, the complexities of these optimization algorithms along with the limited application to symmetrical arrays, switch counts, and complex operations can be potential demerits.

Considering the above limitations, this paper proposed a reliable technique for efficient partial shading dispersion in PV systems, which uses a switching matrix circuit with a minimum number of switches to change the connection to reduce the mismatch and row current difference between modules. The switching matrix provides optimal electrical connection between the modules through a simple particle swarm optimization algorithm for enhancement of power in the PV arrays during partial shading. The proposed system has been analyzed under different partial shading scenarios and compared with the series-parallel (SP), total-cross-tied (TCT), SP-TCT [28], SDS, and FER techniques in MATLAB. The power-voltage (P~V) curves, power output, mismatch loss, MPP counts, and power enhancement have been considered for comparison of the proposed system with other approaches.

II. System under Consideration

In this section, the description of the PV modules rating, system size, conventional and hybrid configurations, existing reconfigurations i.e. SDS [11] and FER [12] and comparative parameters.

A. PV Modules Rating

The rating of the PV modules used in the study has been determined under standard testing conditions of 1000W/m^2 as solar irradiance and 25^{o}C as module operating temperature. The rated maximum power, voltage, and current outputs of the modules are 325W, 37.8V, and 8.59A respectively. Similarly, the open-circuit voltage and short-circuit current of modules are 46.56V and 9.3A respectively.

B. System Size

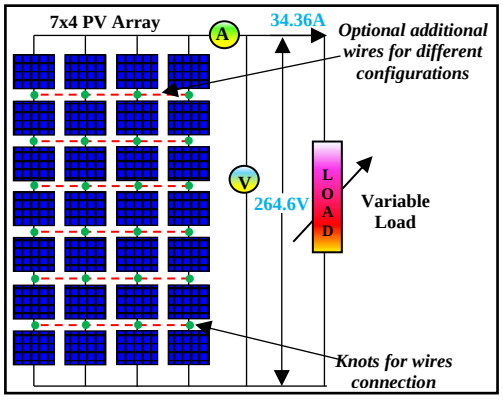

Fig. 2. Schematic representation of the system

Fig.2 shows the schematic representation of the PV system used in the study that consists of a 7x4 PV array with power, voltage, and current output as 9.1 kW, 264.6 V, and 34.36 A respectively at STC. The array is connected to a variable load to plot the power-voltage (P~V) curves using the voltage and current data recorded from the voltmeter and ammeter respectively. Also, it can be seen that extra optional wires are provided along with knots between the connection junctions of the modules to facilitate additional configurations.

C. Array Configurations for Comparison

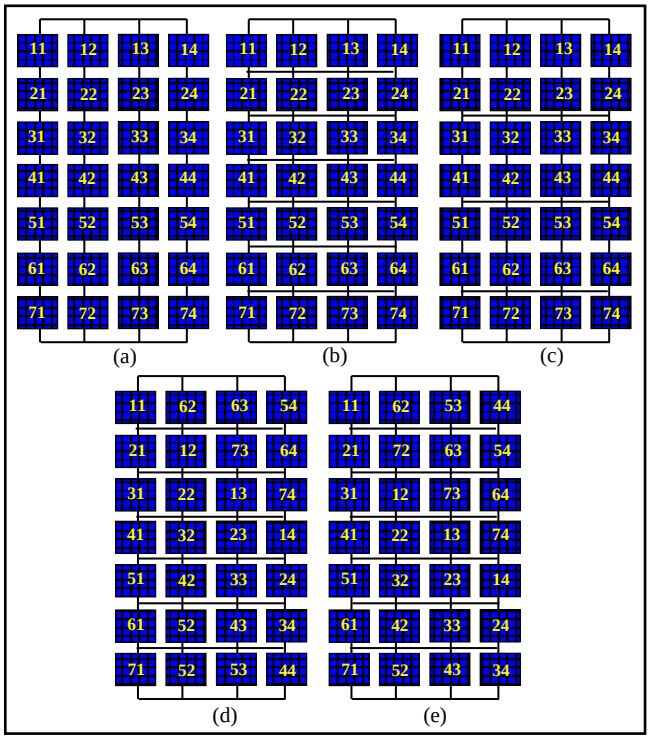

Fig. 3. PV array with different configurations. (a) SP, (b) TCT, (c) SP-TCT, (d) SDS [11], and (e) FER [12]

Fig.3 represents different configurations of the 7x4 array that comprise the SP (Fig.3 (a)), TCT (Fig.3 (b)), SP-TCT (Fig.3 (c)), SDS (Fig.3 (d)) and FER (Fig.3 (e)). The SP is the basic connection of any PV arrays whereas the TCT is formed by connecting additional wires to the junction of the module's connection points. The SP-TCT is formed from hybridization of the SP and TCT connections to reduce the wires count in the array. The SDS and FER are the PV array reconfiguration techniques in which the shading is dispersed throughout the array through a fixed electrical reconnection of the modules.

D. Comparative Parameters

The arrays are compared using output power, power loss, MPP counts, and power enhancement. The power loss (M_{Loss}) can be estimated as

$$P_{Loss} = P_N - P_M \quad (1)$$

The power enhancement (P_E) by the proposed technique as compared to other existing techniques can be calculated as

$$P_E = \frac{P_P - P_{Other}}{P_{Other}} \times 100 \quad (2)$$

III. Genetic Algorithm Based Switching Matrix System

The proposed system has been displayed in Fig.4 which consists of a 7x4 array connected to a switching matrix circuit with 56 inbuilt switches, load, and a switching controller block that contains the particle swarm optimization (PSO) algorithm to generate optimal switching patterns for the switches.

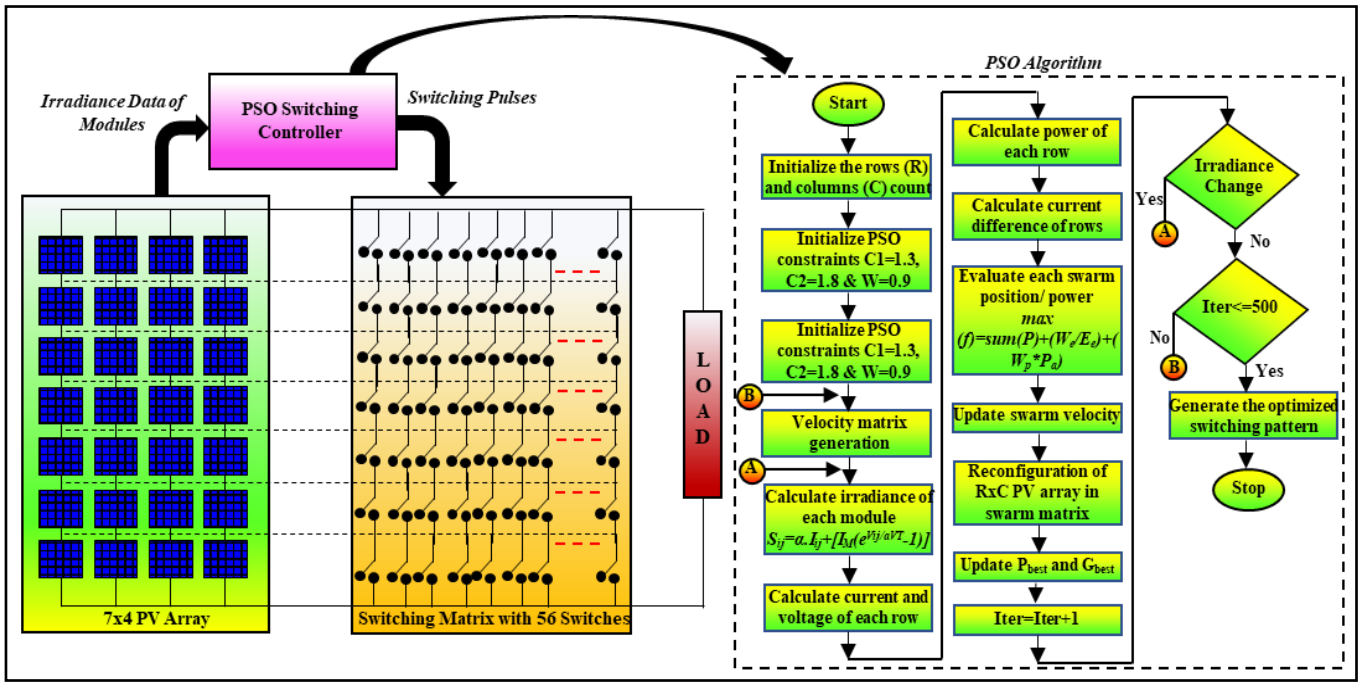

Fig. 4. Schematic representation of the proposed system

The switching controller initially calculates the irradiance levels of individual modules of the array then operates the proposed PSO algorithm to find the optimal switching pattern and accordingly changes the electrical connection among the modules for proper shade dispersion. The PSO algorithm has been used due to various merits such as (a) it can give the best optimal switching pattern for interconnection among modules with effective dispersion of shading even when it starts with from the random movements, (b) robust and easy algorithm, (c) takes less time due to parallel computation, and (d) lower probability of local solution convergence. The steps involved in the operation of the PSO in finding the optimal switching pattern and electrical connection have been explained below.

Step 1: The algorithm initializes inertia weight (W), social (C_1), and cognitive (C_2) constants, row (R), and column (C) counts of the PV array.

Step 2: The algorithm forms a swarm matrix with particles that correspond to the actual *RxC* PV array components. The algorithm generates the swam matrix with the position of the particles stating the initial *RxC* PV array. The initial velocity of the swarms can be calculated using equation (3) where 'k' is the swarm number.

$$V(k) = round(rand() * 8) + 1 \quad (3)$$

Step 3: The array reconfiguration techniques available in the literature require many sensors for irradiance estimation. But, in the proposed system, the irradiance is approximated by utilizing the data from recorded voltage and current of the PV modules using the equation (4) where, 'i', 'j', 'I_{ij}', 'V_{ij}', 'V_T' and 'a' denotes the row index, column index, current output, voltage output, thermal voltage, and ideality factor of the PV modules

$$S_{ij} = \alpha \times I_{ij} + [I_M(e^{\frac{V_{ij}}{aV_T}} - 1] \quad (4)$$

Step 4: The goodness of each particle has been evaluated from the voltage and current values of the modules using the fitness function as

$$\max(f) = Sum(P) + \left(\frac{W_e}{E_e}\right) + (W_p \times P_a) \quad (5)$$

The value of W_e and W_f have been obtained as 10 with a trial-and-error technique. 'P_a' is the power output of each module and *Ee* represents the error between the difference in the row current and particular row current given by equation (6) where 'I_m' and 'I_M' are the maximum current value of R^{th} row, and actual row current respectively.

$$E_e = \sum_{i=1}^{R} |I_m - I_M| \quad (6)$$

Step 5: The swarm velocity has been updated using equation (7) where 'i', 't', '$X_i{}^t$', '$V_i{}^t$', 'C_1' and 'C_2' denotes the vector variable, iteration count, particle position and particle velocity, social and cognitive coefficients respectively. It is to be noted that the velocity of the swarm decreases when they reach the global solution.

$$V_i{}^{t+1} = w \times V_i{}^t + rand \times C_1 \times (P_{best} - X_i{}^t) + rand \times C_2 \times (G_{best} - X_i{}^t) \quad (7)$$

Step 6: The process continues until it meets the stopping condition of getting the optimal switching pattern. However, with the change in the irradiance values of the modules, the algorithm requires reinitialization.

Step 7: Steps 4 to 6 get repeated until the algorithm finds the optimal switching pattern.

After getting the optimal switching pattern, the controller sends the switching pulses to the connected switches in the matrix that changes the electrical connection among modules. It is to be noted that the modules are initially connected in the TCT and continue the same with different interconnections through switches for efficient shade dispersion in the array during partial shading.

IV. Results Analysis and Discussion

The 7x4 PV array with SP, TCT, SP-TCT, SDS, FER, and the proposed system has been tested under four partial shading cases and compared using the power output, losses, power enhancement, and P~V curves.

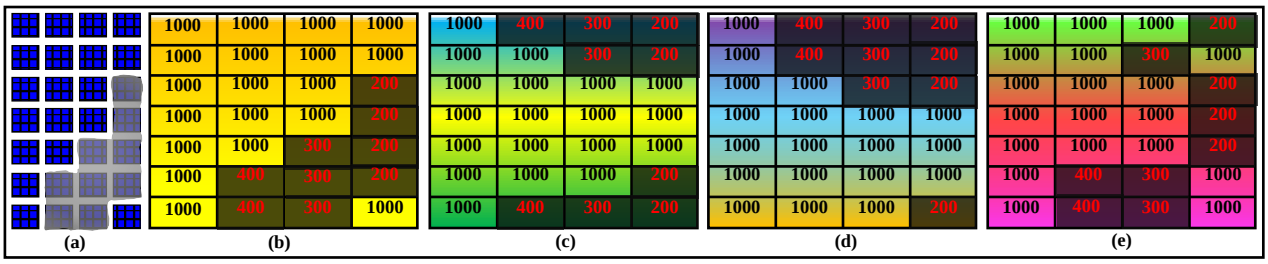

Fig. 5. (a) Partial shading 1 in 7x4 array, (b) irradiance in TCT, and dispersion of shading by (c) SDS [11], (d) FER [12], and (e) proposed system

TABLE I. MATHEMATICAL CALCULATION OF PV ARRAY WITH TCT, SDS, FER, AND PROPOSED SYSTEM DURING PARTIAL SHADING SCENARIO 1

Rows	*TCT*			Rows	*SDS [11]*			Rows	*FER [12]*			Rows	*Proposed System*		
	I	V	P		I	V	P		I	V	P		I	V	P
R6	1.9I_M	7V_M	13.2P_M	**R1**	1.9I_M	7V_M	13.3P_M	**R1**	5.5I_M	7V_M	13.3P_M	**R6**	2.7I_M	7V_M	18.9P_M
R5	2.5I_M	6V_M	15.0P_M	**R7**	1.9I_M	6V_M	11.4P_M	**R2**	5.5I_M	6V_M	11.4P_M	**R7**	3.2I_M	6V_M	19.2P_M
R7	2.7I_M	5V_M	13.5P_M	**R2**	2.5I_M	5V_M	12.5P_M	**R3**	5.6I_M	5V_M	12.5P_M	**R1**	3.2I_M	5V_M	16P_M
R3	3.2I_M	4V_M	12.8P_M	**R6**	3.2I_M	4V_M	12.8P_M	**R7**	5.7I_M	4V_M	12.8P_M	**R3**	3.2I_M	4V_M	12.8P_M
R4	3.2I_M	3V_M	9.6P_M	**R3**	4.0I_M	3V_M	12.0P_M	**R4**	6.1I_M	3V_M	12.0P_M	**R4**	3.2I_M	3V_M	9.6P_M
R1	4.0I_M	2V_M	8.0P_M	**R4**	4.0I_M	2V_M	8.0P_M	**R5**	6.1I_M	2V_M	8.0P_M	**R5**	3.2I_M	2V_M	6.4P_M
R2	4.0I_M	V_M	4P_M	**R5**	4.0I_M	V_M	4.0P_M	**R6**	6.2I_M	V_M	4.0P_M	**R2**	3.3I_M	V_M	3.3P_M

The power output of the system without partial shading at 1000W/m^2 and 25^{o}C has been determined as 9.10kW.

A. *Partial Shading Scenario 1*

The partial shading scenario 1 has been presented in Fig.5 (a) where the shaded PV modules receive irradiance values of 200W/m^2, 300W/m^2, and 400W/m^2. The current output of all the seven rows from the array with TCT connection (Fig.5 (b)) has been presented in equations (8)-(12) as

$$I_{R1} = I_{R2} = 4 \times \frac{1000}{1000} I_M = 4I_M \quad (8)$$

$$I_{R3} = I_{R4} = 3 \times \frac{1000}{1000} I_M + \frac{200}{1000} I_M = 3.2I_M \quad (9)$$

$$I_{R5} = 2 \times \frac{1000}{1000} I_M + \frac{300}{1000} I_M + \frac{200}{1000} I_M = 2.5I_M \quad (10)$$

$$I_{R6} = \frac{1000}{1000} I_M + \frac{400}{1000} I_M + \frac{300}{1000} I_M \frac{200}{1000} I_M = 1.9I_M \quad (11)$$

$$I_{R7} = \frac{1000}{1000} I_M + \frac{400}{1000} I_M + \frac{300}{1000} I_M \frac{1000}{1000} I_M = 2.7I_M \quad (12)$$

The current outputs from different rows of the array with SDS (Fig.5 (c)) after the dispersion of shading through a fixed electrical reconfiguration have been given in equations (14)-(16) as

$$I_{R1} = I_{R7} = 1I_M + 0.4I_M + 0.3I_M + 0.2I_M = 1.9I_M \quad (13)$$

$$I_{R2} = (2 \times I_M) + 0.3I_M + 0.2I_M = 2.5I_M \quad (14)$$

$$I_{R3} = I_{R4} = I_{R5} = 4 \times 1I_M = 4I_M \quad (15)$$

$$I_{R6} = (3 \times 1I_M) + 0.2I_M = 3.2I_M \quad (16)$$

Similarly, the current outputs from rows of the array with FER (Fig.5 (d)) have been given in equations (17)-(20) as

$$I_{R1} = I_{R2} = 1I_M + 0.4I_M + 0.3I_M + 0.2I_M = 1.9I_M \quad (17)$$

$$I_{R3} = (2 \times I_M) + 0.3I_M + 0.2I_M = 2.5I_M \quad (18)$$

$$I_{R4} = I_{R5} = I_{R6} = 4 \times 1I_M = 4I_M \quad (19)$$

$$I_{R7} = (3 \times 1I_M) + 0.2I_M = 3.2I_M \quad (20)$$

The current outputs from different rows after the electrical reconfiguration in the proposed system have been calculated in equations (21)-(24) as

$$I_{R1} = (3 \times 1I_M) + 0.2I_M = 3.2I_M \quad (21)$$

$$I_{R2} = (3 \times 1I_M) + 0.3I_M = 3.3I_M \quad (22)$$

$$I_{R3} = I_{R4} = I_{R5} = (3 \times 1I_M) + 0.2I_M = 3.2I_M \quad (23)$$

$$I_{R6} = I_{R7} = (2 \times 1I_M) + 0.4I_M + 0.3I_M = 2.7I_M \quad (24)$$

It can be observed from the above equations that the TCT, SDS, and FER have the lowest current output values as $1.9I_M$ whereas the value is higher in the case of the proposed system as $2.7I_M$. The overall calculation of voltages and power of the rows for all techniques have been provided in Table I. It is noted that the proposed system has a higher output of $19.2P_M$ than SDS ($13.3P_M$), FER ($13.3P_M$), and TCT ($15P_M$).

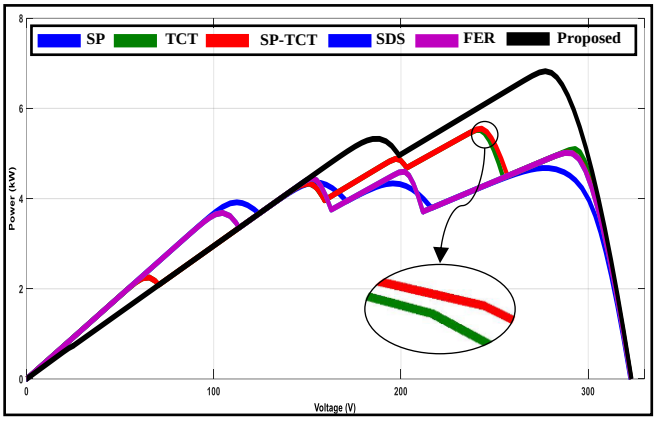

Fig. 6. Array output curves for partial shading 1

The P~V output curves of SP, TCT, SP-TCT, SDS, FER, and the proposed system have been shown in Fig.6. The curve of the proposed system lies at higher power values (6.82kW) with two peaks whereas SP, TCT, SP-TCT, SDS, and FER have maximum power values at 4.67kW, 5.52kW, 5.55kW, 5kW, and 5.01kW respectively. The loss in the proposed system is 2.82kW which is comparatively lower than the SP (4.43kW), TCT (3.58kW), SP-TCT (3.55kW), SDS (4.1kW), and FER (4.09kW). The proposed system is found to have 46.03%, 23.55%, 22.88%, 36.40%, and 36.12% of power enhancement than SP, TCT, SP-TCT, SDS, and FER.

B. *Partial Shading Scenario 2*

The partial shading 2 has been shown in Fig.7 (a) in which the PV array receives lower irradiance values of 100W/m^2, 200W/m^2, 300W/m^2, 500W/m^2 and 600W/m^2. The shading in the case of TCT and dispersion of the shading by SDS, FER, and proposed system are shown in Fig.7 (b)-(d) respectively.

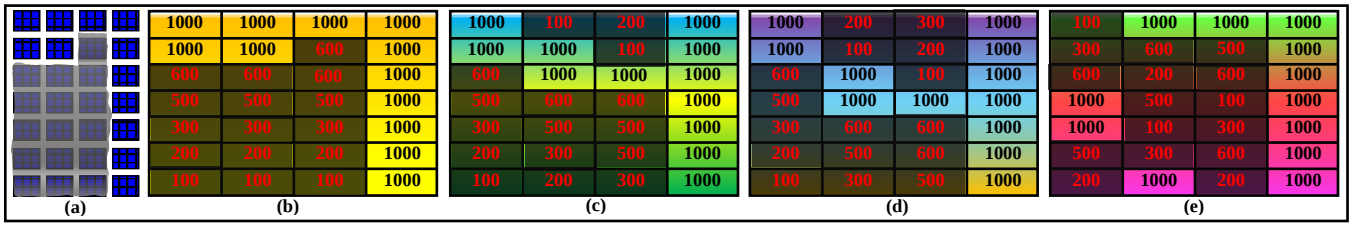

Fig. 7. (a) Partial shading 2 in 7x4 array, (b) irradiance in TCT, and dispersion of shading by (c) SDS [11], (d) FER [12], and (e) proposed system

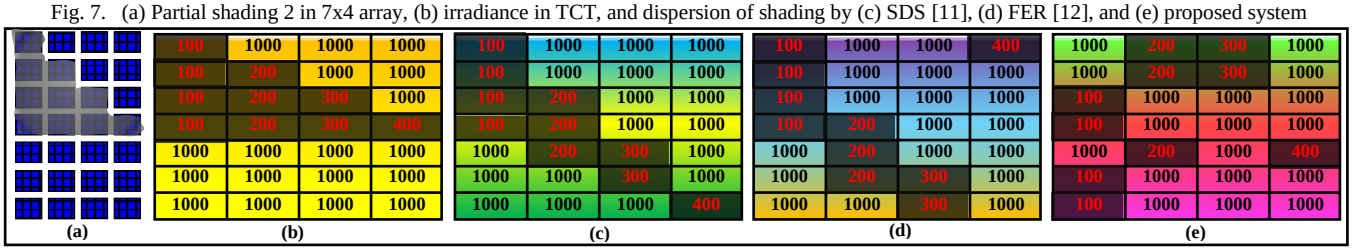

Fig. 8. (a) Partial shading 3 in 7x4 array, (b) irradiance in TCT, and dispersion of shading by (c) SDS [11], (d) FER [12], and (e) proposed system

TABLE II. MATHEMATICAL CALCULATION OF PV ARRAY WITH TCT, SDS, FER, AND PROPOSED SYSTEM DURING PARTIAL SHADING SCENARIO 2

Rows	*TCT*			Rows	*SDS [11]*			Rows	*FER [12]*			Rows	*Proposed System*		
	I	V	P		I	V	P		I	V	P		I	V	P
R7	$1.3I_M$	$7V_M$	$9.1P_M$	R7	$1.6I_M$	$7V_M$	$11.2P_M$	R7	$1.9I_M$	$7V_M$	$13.3P_M$	R2	$2.4I_M$	$7V_M$	$16.8P_M$
R6	$1.6I_M$	$6V_M$	$9.6P_M$	R6	$2.0I_M$	$6V_M$	$12.0P_M$	R2	$2.3I_M$	$6V_M$	$13.8P_M$	R3	$2.4I_M$	$6V_M$	$14.4P_M$
R5	$1.9I_M$	$5V_M$	$9.5P_M$	R1	$2.3I_M$	$5V_M$	$11.5P_M$	R6	$2.3I_M$	$5V_M$	$11.5P_M$	R5	$2.4I_M$	$5V_M$	$12.0P_M$
R4	$2.5I_M$	$4V_M$	$10P_M$	R5	$2.3I_M$	$4V_M$	$9.2P_M$	R1	$2.5I_M$	$4V_M$	$10P_M$	R6	$2.4I_M$	$4V_M$	$9.6P_M$
R3	$2.8I_M$	$3V_M$	$8.4P_M$	R4	$2.7I_M$	$3V_M$	$8.1P_M$	R5	$2.5I_M$	$3V_M$	$7.5P_M$	R7	$2.4I_M$	$3V_M$	$7.2P_M$
R2	$3.6I_M$	$2V_M$	$7.2P_M$	R2	$3.1I_M$	$2V_M$	$6.2P_M$	R3	$2.7I_M$	$2V_M$	$5.4P_M$	R4	$2.6I_M$	$2V_M$	$5.2P_M$
R1	$4.0I_M$	V_M	$4P_M$	R3	$3.6I_M$	V_M	$3.6P_M$	R4	$3.5I_M$	V_M	$3.5P_M$	R1	$3.1I_M$	V_M	$3.1P_M$

TABLE III. MATHEMATICAL CALCULATION OF PV ARRAY WITH TCT, SDS, FER, AND PROPOSED SYSTEM DURING PARTIAL SHADING SCENARIO 3

Rows	*TCT*			Rows	*SDS [11]*			Rows	*FER [12]*			Rows	*Proposed System*		
	I	V	P		I	V	P		I	V	P		I	V	P
R4	$1.0I_M$	$7V_M$	$7.0P_M$	R3	$2.3I_M$	$7V_M$	$16.1P_M$	R4	$2.3I_M$	$7V_M$	$16.1P_M$	R1	$2.5I_M$	$7V_M$	$17.5P_M$
R3	$1.6I_M$	$6V_M$	$9.6P_M$	R4	$2.3I_M$	$6V_M$	$13.8P_M$	R1	$2.5I_M$	$6V_M$	$15.0P_M$	R2	$2.5I_M$	$6V_M$	$15.0P_M$
R2	$2.3I_M$	$5V_M$	$11.5P_M$	R5	$2.5I_M$	$5V_M$	$12.5P_M$	R6	$2.5I_M$	$5V_M$	$12.5P_M$	R5	$2.6I_M$	$5V_M$	$13.0P_M$
R1	$3.1I_M$	$4V_M$	$12.4P_M$	R1	$3.1I_M$	$4V_M$	$12.4P_M$	R2	$3.1I_M$	$4V_M$	$12.4P_M$	R3	$3.1I_M$	$4V_M$	$12.4P_M$
R5	$4.0I_M$	$3V_M$	$12.0P_M$	R2	$3.1I_M$	$3V_M$	$9.3P_M$	R3	$3.1I_M$	$3V_M$	$9.3P_M$	R4	$3.1I_M$	$3V_M$	$9.3P_M$
R6	$4.0I_M$	$2V_M$	$8.0P_M$	R6	$3.3I_M$	$2V_M$	$6.2P_M$	R5	$3.2I_M$	$2V_M$	$6.4P_M$	R6	$3.1I_M$	$2V_M$	$6.2P_M$
R7	$4.0I_M$	V_M	$4P_M$	R7	$3.4I_M$	V_M	$3.4P_M$	R7	$3.3I_M$	V_M	$3.3P_M$	R7	$3.1I_M$	V_M	$3.1P_M$

Table II states the mathematical calculation of currents, voltages, and powers of different rows in which the proposed system has a maximum value($16.8P_M$) than the TCT ($10P_M$), SDS ($12P_M$), and FER ($13.8P_M$). The P~V curves in Fig.9 give the power output of SP, TCT, SP-TCT, SDS, FER, and the proposed system as 3.73kW, 3.65kW, 3.61kW, 4.46kW, 5kW, and 6.02 kW respectively. The power losses in the PV array have been calculated as 2.37kW, 2.45kW, 2.49kW, 1.64kW, 1.1kW, and 0.08kW by SP, TCT, SP-TCT, SDS, FER, and the proposed system respectively. Hence, the proposed system has 61.39%, 64.93%, 66.75%, 34.97%, and 20.40% power enhancement than the SP, TCT, SP-TCT, SDS, and FER respectively.

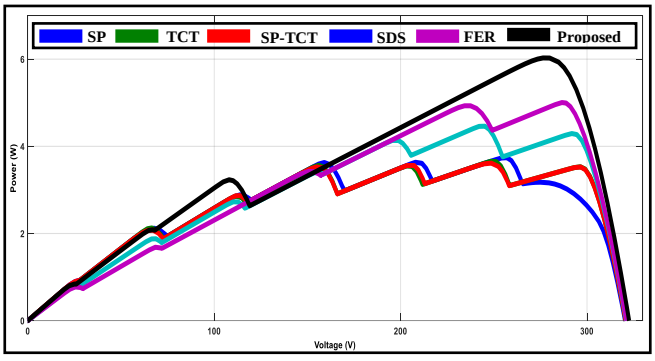

Fig. 9. Array output curves for partial shading 2

C. Partial Shading Scenario 3

Fig.8 (a) shows partial shading scenario 3 in which the shaded modules receive 100W/m^2, 200W/m^2, 300W/m^2, and 400W/m^2. The irradiance values in SP, TCT, and SP-TCT are given in Fig.8 (b) and Fig.8 (c)-(e) showing the dispersion of shading by SDS, FER, and proposed system respectively. The mathematical data in Table III shows the higher power of the proposed system ($17.5P_M$) than the TCT ($12.4P_M$), SDS ($16.1P_M$), and FER ($16.1P_M$).

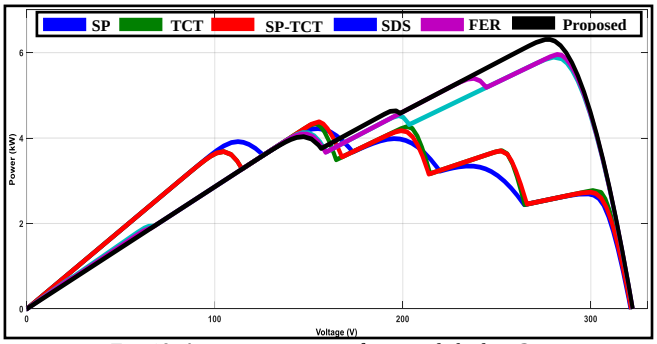

Fig. 10. Array output curves for partial shading 3

The P~V curves in Fig.10 show the higher power output of the proposed system i.e., 5.90kW than SP (3.82kW), TCT (3.93kW), SP-TCT (3.98kW), SDS (5.49kW) and FER (5.55kW). The power losses in the array have been calculated as 2.17kW, 2.12kW, 0.61kW, 0.55kW, 0.5kW and 0.2kW by the SP, TCT, SP-TCT, SDS, FER, and proposed system. The power enhancement by the proposed system over the SP, TCT, SP-TCT, SDS, and FER has been calculated as 54.45%, 50.12%, 48.24%, 7.46%, and 6.30% respectively.

Hence, the conducted analysis in this paper shows higher power output, lower losses, and reduced MPP counts in the

P~V curves of the proposed system than other techniques. Also, the proposed system does not require any sensors and detects the partial shading or irradiance change using the current and voltage data of the modules.

V. CONCLUSION

The system proposed in this paper has been tested using partial shading and performance is compared with SP, TCT, SP-TCT, SDS, and FER techniques. After the investigation, the following conclusions on the merits of the proposed system have been drawn:

- Higher power generation than other techniques under partial shading.
- Mismatch reduction and lower power losses in the array during shading than other techniques.
- Reduction in MPP counts from the P~V curves.
- Average power enhancement of 53.95%, 46.2%, 45.95%, 26.27%, and 20.94% than SP, TCT, SP-TCT, SDS, and FER respectively.
- Higher array performance using reduced switch counts of 56 for 7x4 size.
- Highly reliable than the conventional and static techniques of shading dispersion.
- Cost-effective, less complex, easy to implement, higher efficiency, applicable for all array sizes, and highly reliable technique for partial shading mitigation in PV arrays.

Hence, the proposed system can be an effective solution for loss reduction in the arrays under partial shading. The completion reduction of multiple MPPs from the P~V curves can be the future scope of this work.

REFERENCES

[1] Satpathy, P. R., Sarangi, A., Jena, S., Jena, B., & Sharma, R. (2018, March). Topology alteration for output power maximization in PV arrays under partial shading. In 2018 Technologies for Smart-City Energy Security and Power (ICSESP) (pp. 1-6). IEEE.

[2] Koh, J. S., Tan, R. H., Lim, W. H., & Tan, N. M. (2023). A Modified Particle Swarm Optimization for Efficient Maximum Power Point Tracking under Partial Shading Condition. IEEE Transactions on Sustainable Energy.

[3] Deboucha, H., Kermadi, M., Mekhilef, S., & Belaid, S. L. (2023). Ultra-Fast and Accurate MPPT Control Structure for Mobile PV System under Fast-Changing Atmospheric Conditions. IEEE Transactions on Sustainable Energy.

[4] Satpathy, P. R., Sharma, R., Panigrahi, S. K., & Panda, S. (2020, July). Bypass diodes configurations for mismatch and hotspot reduction in PV modules. In 2020 International Conference on Computational Intelligence for Smart Power System and Sustainable Energy (CISPSSE) (pp. 1-6). IEEE.

[5] Satpathy, P. R., Bhowmik, P., Babu, T. S., Sharma, R., & Sain, C. (2022). Bypass Diodes Configurations for Mismatch Losses Mitigation in Solar PV Modules. In Innovation in Electrical Power Engineering, Communication, and Computing Technology: Proceedings of Second IEPCCT 2021 (pp. 197-208). Springer Singapore.

[6] Nassef, A. M., Houssein, E. H., Helmy, B. E. D., & Rezk, H. (2022). Modified honey badger algorithm based global MPPT for triple-junction solar photovoltaic system under partial shading condition and global optimization. Energy, 254, 124363.

[7] Satpathy, P. R., Babu, T. S., Mahmoud, A. H., Sharma, R., & Nastasi, B. (2021). A TCT-SC hybridized voltage equalizer for partial shading mitigation in PV arrays. IEEE Transactions on Sustainable Energy, 12(4), 2268-2281.

[8] Kishore, D. K., Mohamed, M. R., Sudhakar, K., & Peddakapu, K. (2023). Swarm intelligence-based MPPT design for PV systems under diverse partial shading conditions. Energy, 265, 126366.

[9] Pathy, S., Subramani, C., Sridhar, R., Thamizh Thentral, T. M., & Padmanaban, S. (2019). Nature-inspired MPPT algorithms for partially shaded PV systems: A comparative study. Energies, 12(8), 1451.

[10] Rezazadeh, S., Moradzadeh, A., Pourhossein, K., Akrami, M., Mohammadi-Ivatloo, B., & Anvari-Moghaddam, A. (2022). Photovoltaic array reconfiguration under partial shading conditions for maximum power extraction: A state-of-the-art review and new solution method. Energy Conversion and Management, 258, 115468.

[11] Satpathy, P. R., Sharma, R., & Jena, S. (2017). A shade dispersion interconnection scheme for partially shaded modules in a solar PV array network. Energy, 139, 350-365.

[12] Satpathy, P. R., & Sharma, R. (2019). Power and mismatch losses mitigation by a fixed electrical reconfiguration technique for partially shaded photovoltaic arrays. Energy conversion and management, 192, 52-70.

[13] Amar Raj, R. D., & Anil Naik, K. (2022). A generalized henon map-based solar PV array reconfiguration technique for power augmentation and mismatch mitigation. IETE Journal of Research, 1-19.

[14] Satpathy, P. R., Aljafari, B., & Thanikanti, S. B. (2022). Power losses mitigation through electrical reconfiguration in partial shading prone solar PV arrays. Optik, 259, 168973.

[15] Satpathy, P. R., & Sharma, R. (2018). Power loss reduction in partially shaded PV arrays by a static SDP technique. Energy, 156, 569-585.

[16] Satpathy, P. R., Sharma, R., & Dash, S. (2019). An efficient SD-PAR technique for maximum power generation from modules of partially shaded PV arrays. Energy, 175, 182-194.

[17] Fathy, A., Yousri, D., Babu, T. S., & Rezk, H. (2023). Triple X Sudoku reconfiguration for alleviating shading effect on total-cross-tied PV array. Renewable Energy.

[18] Kansal, I., & Pachauri, R. K. (2023). Game theory-based photovoltaic array system reconfigure method: experimental validation. International Journal of Advanced Technology and Engineering Exploration, 10(99), 202.

[19] Anjum, S., Mukherjee, V., & Mehta, G. (2022). Hyper SuDoKu-based solar photovoltaic array reconfiguration for maximum power enhancement under partial shading conditions. Journal of Energy Resources Technology, 144(3).

[20] Aljafari, B., Satpathy, P. R., Thanikanti, S. B., & Haes Alhelou, H. (2023). A zero switch and sensorless reconfiguration approach for sustainable operation of roof‐top photovoltaic system during partial shading. IET Renewable Power Generation.

[21] Aljafari, B., Satpathy, P. R., Madeti, S. R. K., Vishnuram, P., & Thanikanti, S. B. (2022). Reliability Enhancement of Photovoltaic Systems under Partial Shading through a Two-Step Module Placement Approach. Energies, 15(20), 7766.

[22] Rajani, K., & Ramesh, T. (2020). Maximum power enhancement under partial shadings using a modified Sudoku reconfiguration. CSEE Journal of Power and Energy Systems, 7(6), 1187-1201.

[23] Satpathy, P. R., Bhowmik, P., Babu, T. S., Sain, C., Sharma, R., & Alhelou, H. H. (2022). Performance and reliability improvement of partially shaded PV arrays by one-time electrical reconfiguration. IEEE Access, 10, 46911-46935.

[24] Bouselham, L., Rabhi, A., Hajji, B., & Mellit, A. (2021). Photovoltaic array reconfiguration method based on fuzzy logic and recursive least squares: An experimental validation. Energy, 232, 121107.

[25] Aljafari, B., Satpathy, P. R., & Thanikanti, S. B. (2022). Partial shading mitigation in PV arrays through dragonfly algorithm based dynamic reconfiguration. Energy, 257, 124795.

[26] Zhang, X., Meng, D., Li, W., Yu, T., Fan, Z., & Hao, Z. (2022). Evolutionary based Pareto optimization algorithms for bi-objective PV array reconfiguration under partial shading conditions. Energy Conversion and Management, 271, 116308.

[27] Yousri, D., Allam, D., & Eteiba, M. B. (2020). Optimal photovoltaic array reconfiguration for alleviating the partial shading influence based on a modified harris hawks optimizer. Energy Conversion and Management, 206, 112470.

[28] Satpathy, P. R., Babu, T. S., Shanmugam, S. K., Popavath, L. N., & Alhelou, H. H. (2021). Impact of uneven shading by neighboring buildings and clouds on the conventional and hybrid configurations of roof-top PV arrays. IEEE Access, 9, 139059-139073.